Electronic Supplementary Material (ESI) for Nanoscale.

Amphiphilic Nanoparticles Generate Curvature in Lipid Membranes and Shape Liposome-Liposome Interfaces

E. Lavagna[a], Z. P. Güven[b], D. Bochicchio[a], F. Olgiati[b], F. Stellacci[b] and G. Rossi[a,]*

[a] Physics Department, University of Genoa, Via Dodecaneso 33, 16146 Genoa, Italy

[b] Institute of Materials, Ecole Polytechnique Federale de Lausanne, 1015 Lausanne, Switzerland

AUTHOR INFORMATION

Corresponding Author

[*] rossig@fisica.unige.it

Computational methods

Model In order to simulate samples containing several nanoparticles and liposomes, we relied on the coarse graining provided by Martini force field[4], approximates molecules with a 4 to 1 mapping of the heavy atoms. Martini is parametrized to well describe the properties of the membrane, maintaining lipid specificity while allowing enhanced speed and versatility. Its block building based nature allows to easily implement new molecules or nanoparticles, as it is the case for the Au NP used in this work and their ligand coating.

NP model The model for the NPs had been custom developed for previous works[5–8] using the building blocks of Martini. The core of the NPs was modeled as an hollow sphere with the surface composed of 346 Au and 240 S atoms, with a diameter of 4 nm. A total of 240 ligands are bound to the S atoms of the core: 168 MUS, 72 OT. Topologies of the NPs can be found at this link. The number of Au beads was chosen in order to have a 4 nm diameter core model. The choice of OT content, corresponding to the largest OT content used experimentally, is motivated by its largest affinity with the membrane core which results in a more efficient simulation of NP-membrane interactions. In a previous publication[8], we showed that varying the OT content affects the free energy barriers that characterize the NP-membrane interaction, without altering the overall mechanism of interaction.

Simulations All simulations have been produced via Gromacs 2018.6, using the leap frog molecular dynamics algorithm and the NPT ensemble. We used the so-called velocity rescale[1] temperature coupling, with a reference temperature of 310K. For pressure coupling we used the Berendsen[2] algorithm for equilibration runs (with *tau_p*=4) and the Parrinello Rahaman[3] algorithm for production runs (with

tau_p=12). For membrane simulations, the pressure coupling was semi-isotropic to ensure vanishing surface tension in the bilayers.

Simulated systems

Simulations with liposomes: we setup a system comprising two DOPC liposomes containing 4608 lipids each, incubated with 13 NPs or 0 NPs. The system is solvated in water with 150 mM NaCl. Simulations were run for 10 μs.

Curvature profiles: three different systems, each containing 1 NP and a DOPC bilayer of 2450 lipids, solvated in water with 150 mM NaCl. The different interaction states (adsorbed, semi-snorkeled and symmetrically snorkeled) of the NP with the membrane were obtained putting the NP at the right height relative to the membrane with the INSANE tool and equilibrating for 100 ns.

Unbiased aggregation simulations: we simulated three different systems, again one for each NP-membrane interaction state. 9 NPs were placed on a 3x3 grid and the simulations ran for 10 μs.

Buckling simulations: the starting configurations were extracted from unbiased runs of a bare membrane, or of a membrane with 9 adsorbed or semi-snorkeled NPs after spontaneous aggregation. A 4 bar pressure was applied along the x coordinate using the Parrinello Rahaman barostat with non isotropic coupling.

Jellyfish membrane simulation: we initially prepared a system containing a membrane bicelle of 6050 DOPC lipids, which during the equilibration run closed on itself forming a liposome. A snapshot of this simulation in which the liposome was almost formed was used as starting configuration. The NPs were added at the open edge of the semi-closed liposome. An equilibration run of 10 ns with freezed NPs allowed the membrane edge to envelope the NPs. Then, after an equilibration run of 100 ns, the system was simulated for 5 μs.

Experimental methods

Synthesis of MUS:OT gold nanoparticles with 0-30% OT composition. Gold nanoparticles were synthesized according to the procedure described in our previous publications[9,10]. Briefly, 0.45 mmol of gold salt was dissolved in 200 mL of ethanol and 0.45 mmol of the desired thiol ligand mixture was dissolved in 10 mL of methanol. The two solutions were mixed and stirred for 15 minutes, then a saturated solution of sodium borohydride (13 mmol) was added dropwise. The solution was stirred for two hours and then kept in the fridge (4 ºC) overnight. The nanoparticles were washed 4-5 times with ethanol by centrifugation and finally purified with DI-water using 30kDa Amicon Ultra-15 centrifugal filter devices. At the end of the purification, the concentrated nanoparticles were either precipitated with acetone or freeze-dried.

Characterization of nanoparticles The size distribution of the nanoparticles was determined by transmission electron microscopy (TEM) and the ratio between MUS and OT was determined with nuclear magnetic resonance spectroscopy (^{1}H-NMR), as previously described[9,10].

Liposomes and NP incubation The most abundant lipid in the cell membrane, 1,2-dioleoyl-sn-glycero-3-phosphocholine (DOPC, Avanti Lipids) was used as a model membrane in our studies. Prior to liposome formation, 80 μl of lipid chloroform solution was dried in glass vials inside a desiccator overnight. 200 μl of MilliQ® water was added to hydrate the lipid and the solution was vortexed and sonicated in a bath sonicator until no visible lipid films remained. Small liposomes (diameter 60 nm by DLS) were formed using a probe sonicator which was operated at 40% and 60% amplitudes for 30 s intervals for a total of 3 min. We obtained larger liposomes (> 100 nm) via extrusion of the hydrated lipid solution with 200 nm carbon filters

(Whatman, UK) in mini extruder (Avanti lipids, AL) 21 times. At the end of two methods, liposomes had the concentration of 4 mg/ml (5 mM). Liposomes were kept in a 4 ˚C fridge and used one week after preparation. For cryo imaging ˜2.5 mM of vesicles were incubated with a final concentration of 0.28 mg/ml or 1.4 mg/ml nanoparticles at a final volume of 30 µl at room temperature overnight, without any agitation.

Cryo-EM Grids for cryo-EM and tomograms were prepared in a commercial vitrification system (Vitrobot Mark IV, FEI, Netherlands) with 100% humidity at 22 ˚C. 4 µl of sample was pipetted on the lacey carbon grid (300 mesh, Electron Microscopy Science, Hatfield, PA) which was glow discharged for 3 seconds beforehand. Prior to plunge freezing excess sample was blotted under a blotting force of -15 for 2 seconds. After plunge freezing the grids were transferred at -178 ˚C into a Gatan 626 cryo-holder (Gatan inc. Warrendale, PA) and imaged in a FEI Tecnai F20 microscope (FEI) operated at 200kV. The total electron dose for one image was ˜30 e/Å2 and it was acquired using magnification of 50000X or 62000X (pixel size 0.2 nm and 0.16 nm respectively) with defocus values of -0.8 to -2.4 µm. For stereopair images, tilting angles of ±10˚, ±15˚, ±20˚, or ±30˚were used. Images were recorded by Eagle (2048 x 2048 pixels, FEI) and BM-Ceta camera (4096 x 4096 pixels, FEI). Tomogram was aligned and reconstructed from a tilt series which were mostly acquired between ±60˚ with 2 degree increments. Total electron dose for the tomogram ranged from 30 to 100 e/Å2 and they were acquired using magnification 2900X (0.32 nm) and 50000X (pixel size 0.2 nm) with the defocus value ranging between -3 to -5 µm. Images for tomograms were recorded using a FalconIII camera (4096 x 4096 pixels, FEI), unless otherwise specified. Alignments of the images and reconstructions of the tomograms were done using 3DInspect (FEI).

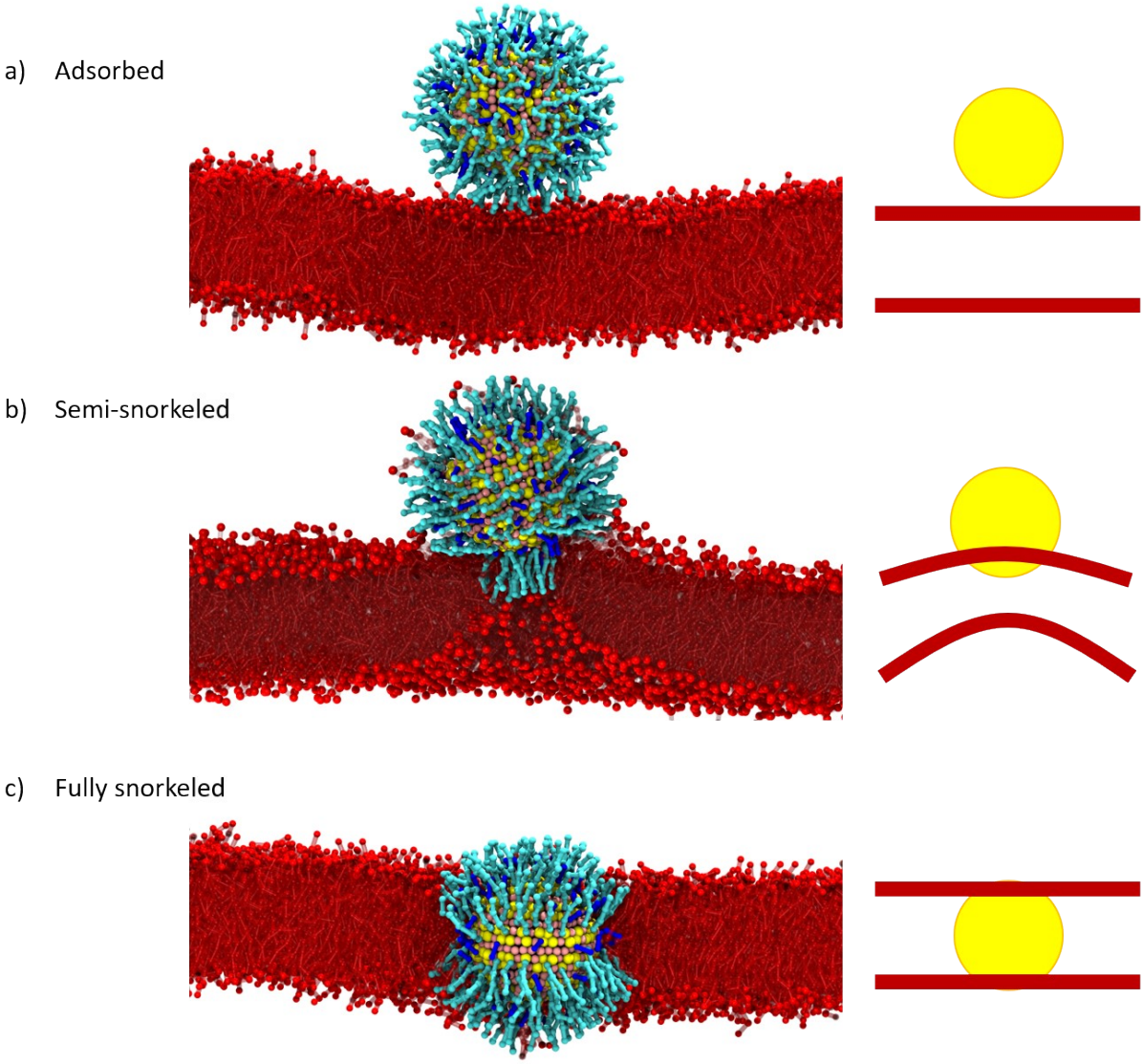

Figure S1: the three insertion steps. a) The adsorbed state. The NP interacts with the membrane surface through the MUS ligands terminals. b) Semi-snorkeled state: few MUS ligands have managed to cross the hydrophobic core of the membrane and are attached to the polar heads of the opposite leaflet. c) Half the ligands have crossed the membrane, displacing the NP at the center of the bilayer. This is the most energetically favourable state of the membrane-NP interaction pathway.

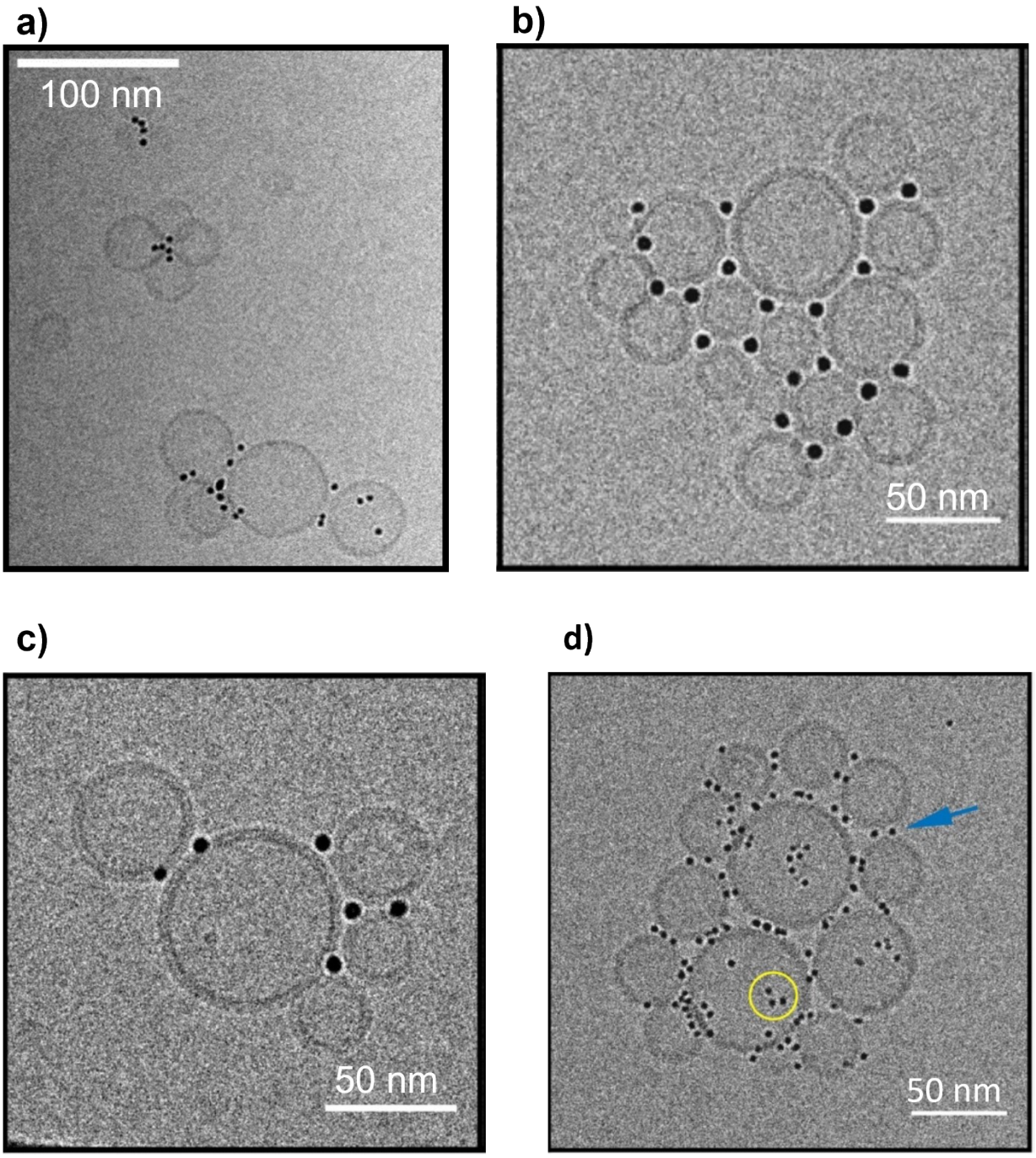

Figure S2 NP mediated liposome clusterization. a) In this cryo-EM image, large liposomes are solvated with NP MUS:OT 10%, size 3.1 ± 0.5 nm. b) and c) Small liposomes and NP MUS:OT 10%, size 5.1 ± 1.5 nm. d) Large liposome and NP allMUS, size 2.7 ± 1.3 nm.

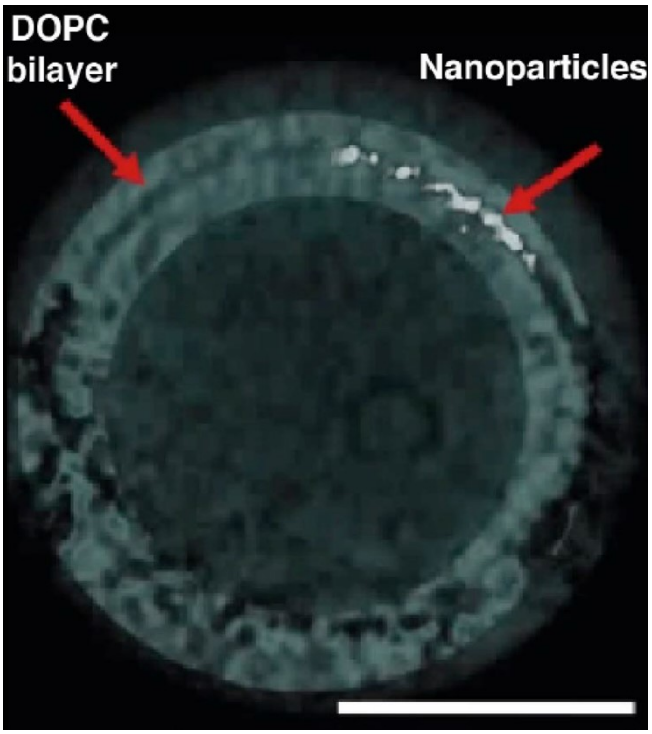

Figure S3. Tomogram reconstruction from cryo-EM images: the NPs are snorkeled and form an aggregate; the scale bar is 100 nm.

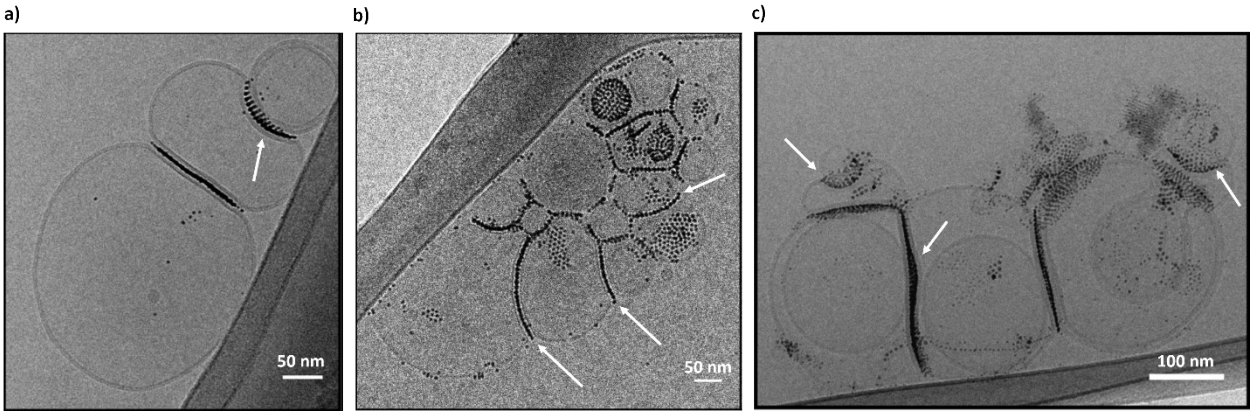

Figure S4. Notable examples of NP-induced negative curvature on DOPC liposomes. a) NP MUS:OT 10%, size 1.7 ± 0.5 nm. b) NP MUS:OT 30%, size 5.0 ± 0.9 nm. c) NP MUS:OT 10%, size 2.8 ± 1.4 nm.

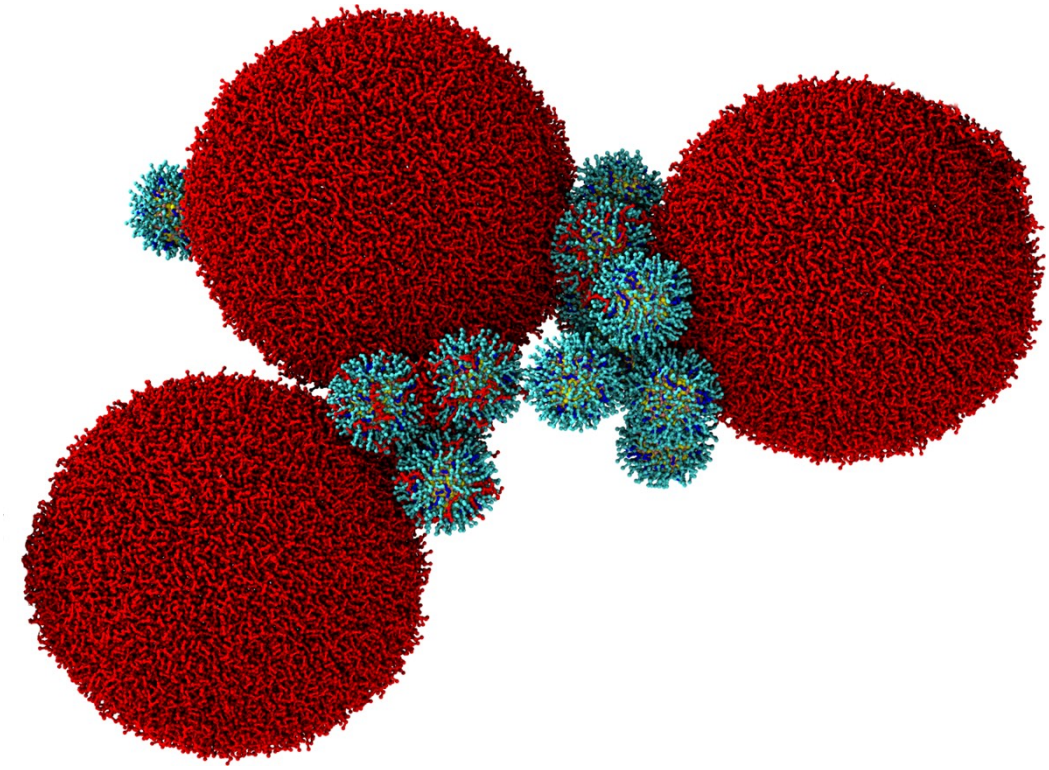

Figure S5. Snapshot of NP-mediated liposome-liposome interaction, obtained from one of the Martini unbiased simulations. Lipid molecules are represented in red, the NP core in pink (Au) and yellow (S), while the ligands are blue (OT) and cyan (MUS). The simulation contains two liposomes, and the ones that we see interacting on the left are doing so through the periodic boundaries.

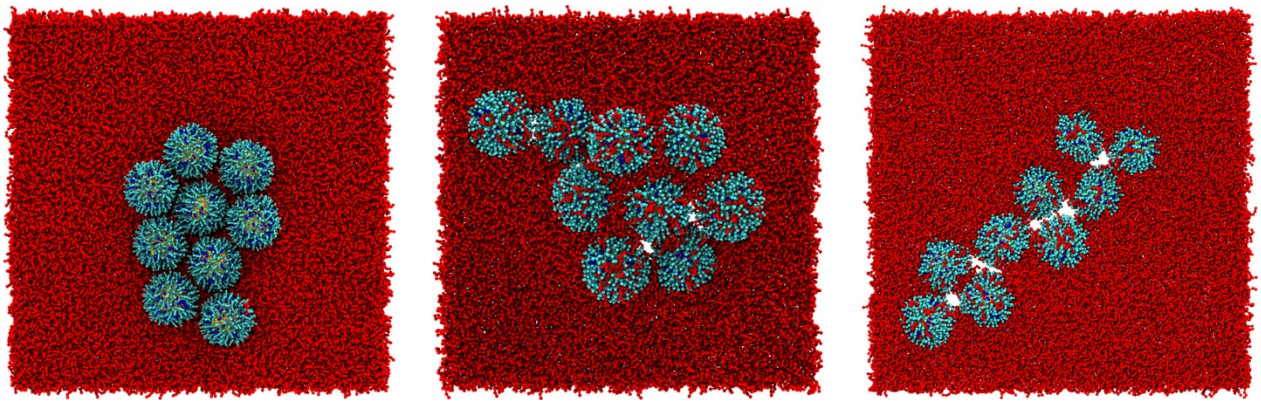

Figure S6. Snapshots of membrane-mediated NP aggregation, for each of the three stages of NP-membrane penetration.

a) Adsorbed NPs:
curvature **sensing**

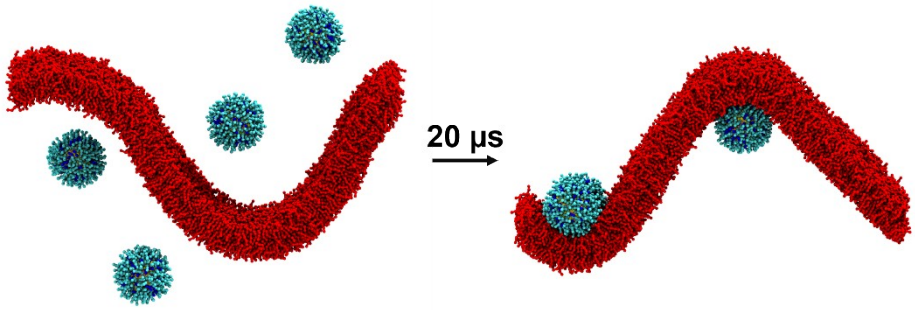

b) Semi-Snorkeled NPs:
inducing local curvature
under stress

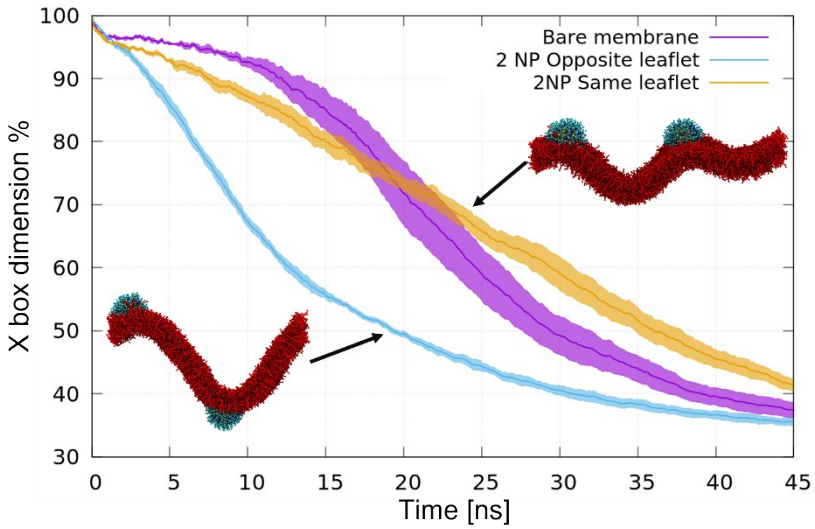

Figure S7. Effects on curvature from isolated NPs. a) Unbiased simulation of four NPs solvated with a buckled DOPC membrane. The buckled configuration of the bilayer is obtained suppressing the compressibility of the box in the x direction. During the run time, all the NPs adhere to the membrane in the regions of maximum negative curvature. b) The membrane reacts differently to stress depending on the position of semi-snorkeled NPs. In the plot, we show the box length reduction vs time, while applying horizontal stress. The NP-bilayer system with NPs on opposite sides bends much faster than the bare membrane, thanks to the NPs that ease the positive curvature. On the contrary, if the NPs are on the same side, the induced curvature is strong enough to force the membrane to buckle with two folds, making it significantly more rigid.

1. Bussi, G., Donadio, D. & Parrinello, M. Canonical sampling through velocity rescaling. *J. Chem. Phys.* **126**, (2007).

2. Berendsen, H. J. C., Postma, J. P. M., Van Gunsteren, W. F., Dinola, A. & Haak, J. R. Molecular dynamics with coupling to an external bath. *J. Chem. Phys.* (1984). doi:10.1063/1.448118

3. Parrinello, M. & Rahman, A. Polymorphic transitions in single crystals: A new molecular dynamics method. *J. Appl. Phys.* **52**, 7182–7190 (1981).

4. Marrink, S. J., Risselada, H. J., Yefimov, S., Tieleman, D. P. & De Vries, A. H. The MARTINI force field: Coarse grained model for biomolecular simulations. *J. Phys. Chem. B* **111**, 7812–7824 (2007).

5. Canepa, E. *et al.* Amphiphilic Gold Nanoparticles Perturb Phase Separation in Multidomain Lipid Membranes. *Nanoscale* (2020). doi:10.1039/d0nr05366j

6. Salassi, S., Canepa, E., Ferrando, R. & Rossi, G. Anionic nanoparticle-lipid membrane interactions: The protonation of anionic ligands at the membrane surface reduces membrane disruption. *RSC Adv.* **9**, 13992–13997 (2019).

7. Salassi, S., Simonelli, F., Bochicchio, D., Ferrando, R. & Rossi, G. Au Nanoparticles in Lipid Bilayers: A Comparison between Atomistic and Coarse-Grained Models. *J. Phys. Chem. C* **121**, 10927–10935 (2017).

8. Simonelli, F., Bochicchio, D., Ferrando, R. & Rossi, G. Monolayer-Protected Anionic Au Nanoparticles Walk into Lipid Membranes Step by Step. *J. Phys. Chem. Lett.* **6**, 3175–3179 (2015).

9. Z. P. Guven, Nanoparticle Liposome Interactions. (EPFL – École polytechnique fédérale de Lausanne, 2018)

10. Guven, Z. P.; Silva, P. H. J.; Luo, Z.; Cendrowska, U. B.; Gasbarri, M.; Jones, S. T.; Stellacci, F. Synthesis and Characterization of Amphiphilic Gold Nanoparticles. *J. Vis. Exp.* **2019**, *2019* (149), 1–11.